Proc. Natl. Acad. Sci. USA
Vol. 93, pp. 7017–7021, July 1996
Biophysics

Three quaternary structures for a single protein

(immunoglobulin light chain/solvent effects/crystal packing contacts)

DE-BIN HUANG, CLINT F. AINSWORTH, FRED J. STEVENS, AND MARIANNE SCHIFFER*

Center for Mechanistic Biology and Biotechnology, Argonne National Laboratory, Argonne, IL 60439-4833

Communicated by Irving M. Klotz, Northwestern University, Evanston, IL, March 11, 1996 (received for review October 15, 1995)

ABSTRACT **The structure of a multisubunit protein (immunoglobulin light chain) was solved in three crystal forms, differing only in the solvent of crystallization. The three structures were obtained at high ionic strength and low pH, high ionic strength and high pH, and low ionic strength and neutral pH. The three resulting "snapshots" of possible structures show that their variable-domain interactions differ, reflecting their stabilities under specific solvent conditions. In the three crystal forms, the variable domains had different rotational and translational relationships, whereas no alteration of the constant domains was found. The critical residues involved in the observed effect of the solvent are tryptophans and histidines located between the two variable domains in the dimeric structure. Tryptophan residues are commonly found in interfaces between proteins and their subunits, and histidines have been implicated in pH-dependent conformation changes. The quaternary structure observed for a multisubunit protein or protein complex in a crystal may be influenced by the interactions of the constituents within the molecule or complex and/or by crystal packing interactions. The comparison of buried surface areas and hydrogen bonds between the domains forming the molecule and between the molecules forming the crystals suggest that, for this system, the interactions within the molecule are most likely the determining factors.**

The immunoglobulin light chain is a multidomain protein; it consists of two domains, the N-terminal variable (V) domain and the C-terminal constant (C) domain. The two domains are connected by a flexible "switch" peptide. Many light chains form dimers by homologous association of the V and C domains of the two chains. The angle between the local twofold axes of the V domain dimer and the C domain dimer defines the "elbow" bend. In antigen binding fragments light chains are associated with heavy chains. The same surface of the light chain domain that is used for formation of antigen binding fragment with heavy chain forms the light chain dimer interface.

We have previously determined the structure of the λ_I type human light chain dimer Loc in two crystal forms (1, 2) crystallized from ammonium sulfate (LocAS) and from distilled water (LocW). We found that the V-domain interactions as well as the elbow bends differed in the two structures. We have now refined these structures using high-resolution data. We have also crystallized the molecule in a third form from $NaKSO_4$ and determined and refined its structure (LocNaKS). This third structure differs from the previous two in the relative positions of the V domains; it appears to be a transition between the two. The three structures allow interpretation of how the solvent of crystallization, its ionic strength, and pH influence the domain interactions in this molecule. The observed modulation of quaternary structures by solvent composition may be relevant to crystallographic analysis of other multidomain proteins as well as protein–ligand and protein–protein complexes.

The publication costs of this article were defrayed in part by page charge payment. This article must therefore be hereby marked "*advertisement*" in accordance with 18 U.S.C. §1734 solely to indicate this fact.

METHODS

LocAS and LocW. The crystallization and the structures of LocAS and LocW determined at 3.0-Å and 2.8-Å resolution, respectively, were described (1, 2). LocAS was grown from 1.8 M $(NH_4)_2SO_4$. We found that we generated LocW crystals more reproducibly if the pH of the dialysis solution was adjusted with $Ca(OH)_2$ to neutrality. High-resolution data for LocAS crystals were collected with the multiwire Xoung type detector at Monsanto, R_{merge} = 3.7%. The LocW high resolution data were obtained from cooled crystals (4°C) by using a Siemens detector at Argonne National Laboratory, R_{merge} = 4.5%. Simulated annealing refinement was carried out by using the program X-PLOR (3) with the new reflections and the previously determined coordinates. At the end of this refinement cycle, the R factor was 27% for LocAS and 26% for LocW. Both structures were rebuilt from "omit" maps by excluding 20 residues at a time; manual adjustments were performed on an Evans & Sutherland (Salt Lake City) model PS300 color graphics system, using the computer program FRODO (4). After several cycles of manual adjustments and restrained least-squares refinement with the refinement program PROLSQ (5), the R factors decreased to 24% and 23% with overall temperature factors. After the introduction of individual temperature factors the R factors further decreased to 22% and 21% respectively. At this point water molecules were introduced; first the occupancies and then the temperature factors of the waters were varied. The final water occupancies ranged from 0.4 to 1.0; their B-values were <56 Å^2 for 364 waters in LocAS and <46 Å^2 for 264 waters in LocW. At the end of the refinement, the R factor for 14,539 reflections of LocAS with $F_o > 3\sigma F$ between 10- and 2.4-Å resolution was 16.5%, and 15.5% for 10,327 reflections of LocW with $F_o > 3\sigma F$ between 10- and 2.4-Å resolution. The details of the refinement are shown in Table 1.

LocNaKS. The third form of Loc, LocNaKS, was crystallized from 0.95 M Na_2SO_4 and 0.4 M K_2SO_4 in 0.04 M phosphate at pH 8. The crystals were orthorhombic $P2_12_12_1$ with the following unit cell dimensions: a = 83.87 Å, b = 72.62 Å, and c = 63.56 Å. Diffraction data were collected on a Picker diffractometer with a Krisel Control system at room temperature. The Krisel Control software was modified by F.J.S. and C.F.A. (unpublished results). Four crystals were used for the data collection. After absorption correction and linear decay correction were applied, the R factors between the different data sets were between 3.2 to 4.7%. A total of 18,459 independent reflections were obtained between 25.6- and 2.2-Å resolution.

Abbreviations: V, variable; C, constant.

Data deposition: The atomic coordinates and structure factors have been deposited in the Protein Data Bank, Chemistry Department, Brookhaven National Laboratory, Upton, NY, 11973 (references: for LocAS, 3BJL and R3BJLSF; for LocW, 4BJL and T4BJLSF; and for LocNaKS, 1BJM and R1BJMSF).

*To whom reprint requests should be addressed.

Table 1. Structural and refinement data for the three crystal forms of protein Loc

	LocAS*	LocW†	LocNaKS‡
Space group	$P2_12_12_1$	$P2_12_12_1$	$P2_12_12_1$
a, Å	149.3	118.9	83.9
b, Å	72.4	73.6	72.6
c, Å	46.5	49.8	63.6
Volume fraction of protein	0.45	0.52	0.58
Resolution, Å	2.4	2.4	2.2
No. of reflections, $>3\sigma F$	14,539	10,327	14,084
No. of waters	364§	264	298§
R factor, %	16.5	15.5	15.9
Deviations in			
Bond length, Å	0.016	0.016	0.017
Angle-related distance, Å	0.044	0.043	0.043
Deviation from plane, Å	0.013	0.013	0.014
Chiral volume, Å^3	0.190	0.179	0.193

*Crystallized from 1.4 M $(NH_4)_2SO_4$.
†Crystallized from distilled water.
‡Crystallized from 0.95 M Na_2SO_4, 0.4 M K_2SO_4, and 0.04 M Na_3PO_4.
§No sulfate ions found.

The structure was determined by molecular replacement by using the program package MERLOT (6) with a modified LocAS structure, where the elbow angle was altered by 8°, as the search model. For the search, 8- to 3.5-Å data were used, and the Patterson search radius was 24 Å; the rotation peak height was 5.3 times background. The location of the molecule was determined from two Harker sections. The orientations of the four domains were first refined by rigid body refinement with the X-PLOR program reducing the *R* factor from 48 to 42% for 8- to 3-Å data. This was followed by simulated annealing refinement by using the SLOWCOOL option of X-PLOR (3), the *R* factor decreased to 31% for 10- to 2.2-Å data. After several cycles of rebuilding and least-squares refinement by PROLSQ (5) the structure refined to 24% with overall temperature factors and to 22% with individual temperature factors. A total of 298 water molecules were located with $B < 47Å^2$ and occupancies between 0.4 and 1.0. The final *R* factor was 15.9% for 14,084 reflections with $F_o > 3\sigma F$ between 10.0- and 2.2-Å resolution. The average temperature factor was 23 Å^2 for protein atoms and 27 Å^2 for waters.

The coordinates and structure factors for the three structures have been deposited in the Protein Data Bank at Brookhaven National Laboratory.

RESULTS

Description of Structures. Except for some variation in the complementarity-determining regions and other loops, the conformations of the domains, based on the comparison of α-carbon coordinates, are the same in the three structures (average rms deviation is 0.6 Å). Therefore, the intradomain arrangement of β-sheets and the curvature of the V-domain faces do not change. The molecular geometries are summarized in Table 2. While the interactions of the V domain changes, as discussed below in detail, the interactions between the C domains are essentially the same in all three crystal forms. The elbow bend is similar for the two high-salt forms (≈97°) and differs from the low-salt form, which has an elbow bend of 120°. This difference between the three forms is correlated with variation in the phi-psi angles of the switch peptides that form the elbow bend and is essentially localized to five residues. In one of the chains, monomer 2, the V and C domains are farther from each other than in monomer 1. In all three dimers, monomer 1 has the ball-and-socket joint previously described for heavy chains in Fab fragments (7); heavy chain residues Ser-112 and Phe-149 are replaced by Leu and by Tyr in the Loc light chain.

Table 2. Description of the structural relationship of domains

	LocAS	LocW	LocNaKS
Elbow bend, °	96.7	119.3	97.6
Rotational sym (°), V domains	179.9	180.0	179.8
Translation of V domains, Å	3.5	0	1.0
Rotational sym (°), C domains	178.4	178.7	177.3
Translation of C domains, Å	0.2	0.2	0.2

Variable Domain Geometries. The V-domain interactions are different in the three forms; the differences in V-domain dimer geometries are illustrated in Fig. 1 in which the V domains of monomer 1 in each crystal form are superimposed. The differences are also shown in Table 3, which gives the rotation and translation that is required to superimpose the V domains of monomer 1 following the superposition of the V domains of monomer 2 of each molecule. The two V domains are related by a local twofold axis in LocW, but by local twofold screw axes with 1- and 3.5-Å screw components in LocNaKS and LocAS, respectively. In both high-salt forms, the V domain of monomer 2 is translated forward, away from the C domain, along the local twofold screw axis relative to the other V domain. There is one hydrogen bond between the V domains of LocAS, two between the V domains of Loc W, and four between the V domains of LocNaKS, as illustrated in Fig. 2.

In the two high-salt forms, Trp-91 residues from both monomers are close together at the interface, while in the low-salt form the two V domains form a more "open" conformation in which the Trp-91 residues are distant from each other, as shown in Fig. 3. The arrangement of the V domains of LocW is most similar, though not identical (2), to that which was observed for Mcg, another λ light-chain dimer crystallized from ammonium sulfate (10). In both structures, the V domains are related by a local twofold axis, and the side chains of residues 91 (Tyr in the Mcg protein) are not in contact with each other. The Mcg V-dimer structure is closely related to the Fab structures (10) for which the interaction of the two V domains was described as an eight-stranded barrel that has a

FIG. 1. Superposition of monomer 1 variable domains of the three structures illustrates the differences in the relative positions of the domains. The three crystal forms are LocAS (white), LocNaKS (blue), and LocW (red). The figure was made by using the program SETOR (8).

Table 3. Comparison of V-domain interaction geometries of the Mcg protein and the three Loc structures

	LocAS		LocW		LocNaKS	
	Degrees	Translation, Å	Degrees	Translation, Å	Degrees	Translation, Å
Mcg	36.9	4.9	16.8	3.2	24.6	3.3
LocAS			38.3	2.4	20.4	2.5
LocW					17.9	0.7

The table lists the absolute value of the rotation and translation calculated on the basis of the procedure of Colman et al. (9) to compare interaction geometries of V–V domains. For the superposition of the domains, α-carbon coordinates of 26 residues in the V–V interface were used. These residues are 33–39, 43–47, 84–90, and 98–104.

"three-layer packing" (11). In the high-salt forms, especially in LocAS, the barrel formed by the two V domains is distorted. Its size is smaller and it is asymmetric because of the screw axis relationship between the two domains, which decreases the separation between two of the strands of monomer 1 and the concave surface of monomer 2. The smaller barrel in the high-salt forms makes possible the hydrogen bond observed between Tyr-336 (Tyr-36 of the second monomer) and the main chain of residue 96. The motion of the V domains that interconverts the different V-dimer geometries we observe can be considered as a shear mechanism (12), while the relative positions of the V and C domains are reflected by the elbow bend, which is changed by a concerted hinge motion of the two chains.

Description of Crystal Contacts. Although the unit-cell dimensions, V domain geometries, and elbow bends differ, the interactions of the C domains in the crystal lattice are conserved in the three crystal forms. A twofold screw axis along the *b* axis of the crystal relates the constant domains to each other. A six-chain β-pleated sheet structure is formed from the three-chain layer of the C domains by the local twofold axis that is perpendicular to the *b* axis. This energetically favorable "infinite" β-sheet arrangement was previously observed and appears to be a significant factor in the formation of λ-type light chain crystals (13).

Table 4 summarizes the buried surface areas and the numbers of hydrogen bonds (including salt bridges) between the domains of each molecule and between the molecules in the different crystals. The buried surface area in the individual crystal contact range from 360 to 1570 Å^2 (LocAS, 360-1540 Å^2; LocW, 410-1430 Å^2; and LocNaKS, 410-1570 Å^2). There is approximately one polar interaction per 200 Å^2 of buried surface area, as was previously observed for pancreatic ribonuclease crystal forms (15). In the two high-salt crystal forms, the buried surface area is larger between the two V domains, and also in the "elbow," than in the low ionic strength form. The low ionic strength form also buries less surface in the crystal contacts. Comparing the area buried within the molecule and in the crystal contacts, more area is buried in the formation of each individual light chain dimer from its constituent domains than is buried between the molecules forming the crystal. The trend shown by the distribution of hydrogen bonds is not clear. With a 3.5-Å cutoff, LocAS and LocW have more hydrogen bonds in the crystal packing contacts than between the domains of each molecule; this trend is reversed when the cutoff is changed to 3.2 Å. Therefore, it appears that, on average, the hydrogen bonds between neighboring molecules of the crystal lattice are weaker than the ones between the domains within the molecule. In each form, one interdomain and one intermolecular salt bridge is observed; therefore, their effects cancel out. Water bridges were not considered, since the numbers of water molecules identified differed in the three structures.

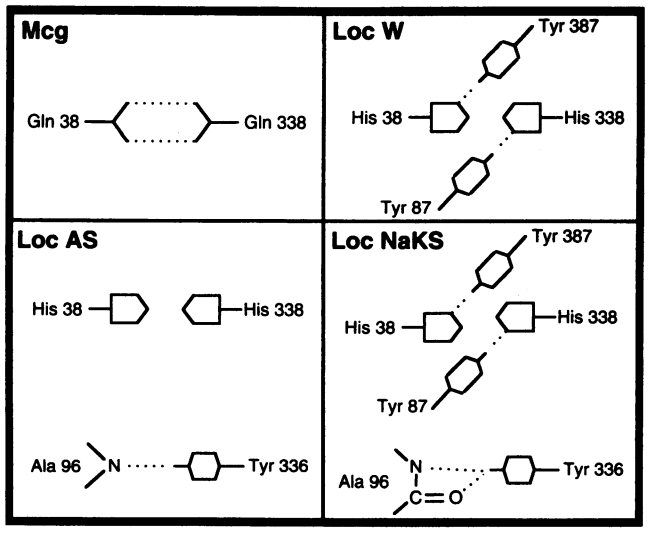

FIG. 2. Schematic illustration of the hydrogen bonds formed by residue 38 in LocW, LocAS, LocNaKS, and, for comparison, in the Mcg crystal. Additional hydrogen bonds found in the interface of Loc crystals are also shown. Three hundred was added to the residue numbers of chain 2. The crystals of LocAS were grown at pH < 6.0 where the histidine residues are not expected to be ionized, while LocW and LocNaKS were grown at pH ≥ 7.0 where they are expected to be ionized.

DISCUSSION

On the basis of the first two crystal forms analyzed, LocAS and LocW, we speculated that the V-domain interactions were driven by the high-salt conditions, which could favor the hydrophobic interactions between Trp-91 residues from both chains (2). Indeed, as expected, in the second high-salt form (LocNaKS), the relative positions of the two tryptophans are very similar to those found in LocAS. What we discovered by solving the structure of the third crystal form is that in addition to the difference in ionic strength, the pH at which the crystals were grown also contributed to these quaternary structures achieved by protein Loc. The pH of LocAS was less than 6, while the pH of LocW was adjusted to neutral pH with $Ca(OH)_2$, and LocNaKS was grown at pH 8.0. In the Loc protein the usual glutamine residue at position 38 is replaced by a histidine residue. The pH of crystallization presumably influences the ionization state of histidine 38 residue, because the pK_a of histidine residues in proteins is between 6.5 and 7.0. Indeed, in crystals grown at pH 7 and above, both at low ionic strength (LocW) and at high ionic strength (LocNaKS), His-38 is involved in hydrogen-bonding interactions with Tyr-87 of the other monomer. His-38 is not expected to be ionized in LocAS, at pH less than 6, and is indeed not involved in any hydrogen-bonding interactions.

Gln-38 (or its equivalent, Gln-39, in the heavy chain) forms hydrogen bonds across the V-domain dimer interface with the equivalent Gln from the other chain. Gln at framework position 38 occurs in over 90% of all light chains; the next most common residue at that position is His (16). Hydrogen bonds involving residue 38 for the three Loc structures and for the Mcg protein (where 38 is a Gln residue) are shown schemat-

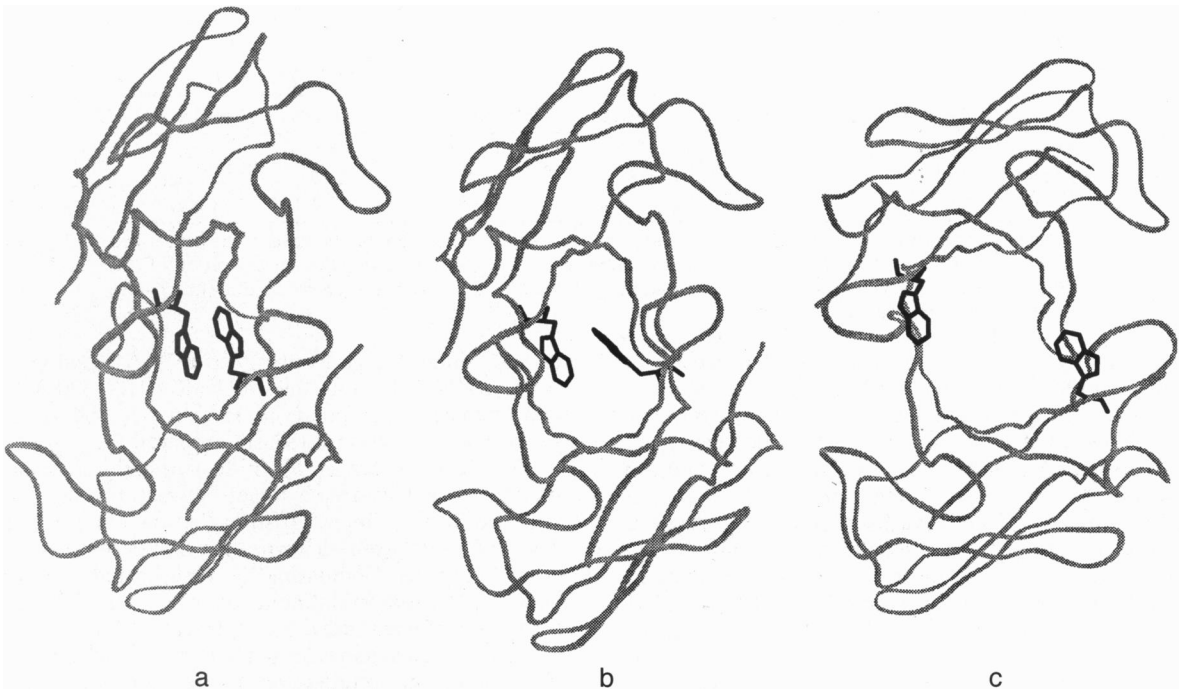

FIG. 3. The backbones of the three variable domain structures with the position of Trp-91 of both monomers illustrated, looking along the local twofold axis: LocAS (*a*), LocNaKS (*b*), and LocW (*c*). In the two high-salt forms, the tryptophans are close together, while they are distant in the low-salt form.

ically in Fig. 2. The ionization of the histidine and the resulting change of its hydrogen-bonding potential appear to trigger the rearrangement of the interactions of the V domains in LocAS that leads to the LocW conformation and crystal form at low ionic strength and to the LocNaKS conformation and crystal form at high ionic strength. A pH "trigger" has been suggested to be involved in switching between two crystal forms of basic pancreatic trypsin inhibitor (BPTI) (17). Major rearrangements caused by pH change have been observed in several systems (18, 19). These rearrangements might have been affected by the change of ionization state of His residues, since there are His residues in or close to the segments where the rearrangement occurs. Apparent changes in the ionization of His residues are also implicated in several allosteric proteins (see ref. 20 for a review).

In the interfaces between the two Loc V domains, there appear to be two groups, His-38 and Trp-91, located at the two ends of the interface, that influence the quaternary structures obtained by the domains in the different crystallization conditions. Despite differences in interaction, in all three Loc dimers, a series of conserved aromatic residues forms a herringbone pattern in the middle of the variable domain interface, as has been described in Fab fragments (21). Trp-91 and His-38 are above and below these residues along the local twofold axis. In other multisubunit proteins, Trp and His residues, together with Phe and Tyr, occur as frequently in the subunit or domain interfaces as in their interiors (22, 23). High ionic strength favors hydrophobic interactions and, therefore, the maximization of buried surface area that we observe in LocAS and LocNaKS relative to LocW. In the high-salt forms, the Trp residues at position 91 are mostly buried in the interface, resulting in juxtaposition of the indole rings that are sequestered from solvent; therefore, the electrostatic interactions (24) between Trp-91 residues of the two domains are optimized.

Table 4. Comparison of buried surface areas and hydrogen bonds

	LocAS		LocW		LocNaKS	
	BS, Å^2	No. HB	BS, Å^2	No. HB	BS, Å^2	No. HB
Within the molecule						
V1–V2	1530	1 (1)	1212	2 (1)	1682	4 (3)
C1–C2	2154	12 (9)	2315	13 (9)	2418	20 (12)
In elbow	1550	2 (1)	1283	4 (3)	1618	7 (2)
Total	5234	15 (11)	4810	19 (13)	5718	31 (17)
% of domains buried	21.9		20.0		23.7	
Crystal contacts						
Total	4016	24 (12)	3576	22 (11)	4585	19 (12)
% of molecule buried	21.5		18.7		24.9	

The hydrogen bonds (HB) include salt bridges; they were calculated with $d < 3.5$ Å and with $d < 3.2$ Å, shown in parenthesis. The buried surface area (BS) was calculated with a 1.4-Å radius probe, with a computer program written by M. D. Handschumacher and F. M. Richards (14).

The quaternary structure observed for a multisubunit protein or protein complex in a crystal may be influenced by the interactions of the constituents within the molecule or complex and/or by crystal packing interactions. Our results suggest that the differences in molecular structure observed in the three crystal forms of protein Loc grown in various solvent conditions are predominantly generated by differences between the domain interactions instead of contacts between molecules in the crystal lattice.

In all three crystal forms the buried surface area between the domains is 1100–1200 Å^2 larger than in the packing contacts. To a first approximation, the free energy of interaction between two macromolecules is proportional to the area of surface that is buried upon formation of the complex. Using the factor of 24 cal/mol per Å^2 (25), which implicitly incorporates an averaged contribution of hydrogen bonds, salt bridges, and van der Waals contacts, the energy of interaction between the domains of the molecule is 26.4–28.8 kcal/mol larger than the energy involved in the interactions between a molecule and its neighbors in the crystal lattice.

Intra- and intermolecular (crystal) energetics might also be estimated by explicitly enumerating the specific interactions. By using a generous hydrogen bond cut-off of 3.5 Å, the LocAS crystal has an additional nine hydrogen bonds that could

account for ≈4.5–13.5 kcal/mol by using an estimate of 0.5–1.5 kcal/mol per hydrogen bond (26). Because most of the excess hydrogen bonds are longer than 3.2 Å, the actual energy involved is likely to be on the low side of this estimate. By using a 9 cal/mol per Å^2 for the energy contribution of surface area, when hydrogen bonds and salt bridges are excluded (27), the excess buried surface within the molecule in LocAS crystal accounts for 11 kcal/mol. In the LocW and LocNaKS crystals, hydrogen bonds involved in formation of the molecule and lattice formation are comparable in number. Thus, although both intra- and intermolecular interactions contribute to the arrangement of domains in the three crystal forms, in each of these cases it appears reasonable to infer that the interfacial energetics of the molecule is the major determinant of the observed quaternary interactions.

The possibility of the functional importance of relative movement (9, 28) of the two variable domains was suggested crystallographically in comparisons of Fab structures with or without bound antigen (29, 30). The contribution of isomerism to the dynamics of antibody interactions was confirmed recently by Foote and Milstein (31). Multiple relative positions of V domains in Fab structures should be possible and may provide a significant contribution to antibody diversity (28). For the Loc molecule, at least three forms from the available repertoire can be crystallized. The conserved C-domain packing in the λ light chain crystal facilitates their crystallization regardless of the V-domain packing (13). Therefore, these two domain molecules, in both native and recombinant forms, offer a versatile system for study of fundamental structural and solvent contributions to the quaternary organization of proteins in general.

We thank Drs. Chong-Hwan Chang and Huey-Sheng Shieh for collecting the diffraction data, George Johnson for the structural figures, and Dr. Deborah K. Hanson for critically reading the manuscript. This work is supported by the U.S. Department of Energy, Office of Health and Environmental Research, under Contract No. W-31-109-ENG-38, and by the U.S. Public Health Service Grant DK 43757. This research was also supported in part by a grant from the Pittsburgh Supercomputing Center through the National Institutes of Health National Center for Research Resources cooperative agreement.

1. Chang, C.-H., Short, M. T., Westholm, F. A., Stevens, F. J., Wang, B.-C., Furey, W., Jr., Solomon, A. & Schiffer, M. (1985) *Biochemistry* **24,** 4890–4897.
2. Schiffer, M., Ainsworth, C., Xu, Z.-B., Carperos, W., Olsen, K., Solomon, A., Stevens, F. J. & Chang, C.-H. (1988) *Biochemistry* **28,** 4066–4072.
3. Brunger, A. T. (1992) X-PLOR: A System for X-Ray Crystallography and NMR (Yale Univ. Press, New Haven, CT), Version 3.1.
4. Jones, T. A. (1978) *J. Appl. Crystallogr.* **11,** 268–272.
5. Hendrickson, W. (1985) *Methods Enzymol.* **115,** 252–270.
6. Fitzgerald, P. M. D. (1988) *J. Appl. Crystallogr.* **21,** 273–278.
7. Lesk, A. M. & Chothia, C. (1988) *Nature (London)* **335,** 188–190.
8. Evans, S. V. (1990) *J. Mol. Graphics* **11,** 134–138.
9. Colman, P. M., Laver, W. G., Varghese, J. H., Baker, A. T., Tulloch, P. A., Air, G. M. & Webster, R. G. (1987) *Nature (London)* **326,** 358–363.
10. Schiffer, M., Girling, R. L., Ely K. R. & Edmundson, A. B. (1973) *Biochemistry* **12,** 4620–4631.
11. Chothia, C., Novotný, J., Bruccoleri, R. & Karplus, M. (1985) *J. Mol. Biol.* **186,** 651–663.
12. Gerstein, M., Lesk, A. M. & Chothia, C. (1994) *Biochemistry* **33,** 6739–6749.
13. Schiffer, M., Chang, C.-H. & Stevens, J. F. (1985) *J. Mol. Biol.* **186,** 475–478.
14. Lee, B. & Richards, F. M. (1971) *J. Mol. Biol.* **55,** 379–400.
15. Crosio, M.-P., Janin, J. & Jullien, M. (1992) *J. Mol. Biol.* **228,** 243–251.
16. Kabat, E. A., Wu, T. T., Perry, H. M., Gottesman, K. S. & Foeller, C., eds. (1991) *Sequences of Proteins of Immunological Interest* (National Institutes of Health, Bethesda, MD), 5th Ed.
17. Gallagher, W. H. & Croker, K. M. (1994) *Protein Sci.* **3,** 1602–1604.
18. Bullough P. A., Hughson, F. M., Skehel, J. J. & Wiley, D. C. (1994) *Nature (London)* **371,** 37–43.
19. Bennett, M. J., Choe, S. & Eisenberg, D. (1994) *Proc. Natl. Acad. Sci. USA* **91,** 3127–3131.
20. Perutz, M. F. (1989) *Q. Rev. Biophys.* **22,** 139–236.
21. Novotný, J. & Haber, E. (1985) *Proc. Natl. Acad. Sci. USA* **82,** 4592–4596.
22. Argos, P. (1988) *Protein Eng.* **2,** 101–113.
23. Janin, J., Miller, S. & Chothia, C. (1988) *J. Mol. Biol.* **204,** 155–164.
24. Burley, S. K. & Petsko, G. A. (1988) *Adv. Protein Chem.* **39,** 125–189.
25. Chothia, C. (1974) *Nature (London)* **248,** 338–339.
26. Fersht, A. R., Shi, J.-P., Knill-Jones, J., Lowe, D. M., Wilkinson, A. J., Blow, D. M., Brick, P., Carter, P., Waye, M. M. Y. & Winter, G. (1985) *Nature (London)* **314,** 235- 238.
27. Schiffer, M., Chang, C.-H., Naik, V. M. & Stevens, F. J. (1988) *J. Mol. Biol.* **203,** 799–802.
28. Stevens, F. J., Chang, C.-H. & Schiffer, M. (1988) *Proc. Natl. Acad. Sci. USA* **85,** 6895–6899.
29. Bhat, T. N., Bentley, G. A., Fischmann, T. O., Boulot, G. & Poljak, R. J. (1990) *Nature (London)* **347,** 483–485.
30. Stanfield, R. L., Takimoto-Kamimura, M., Rini, J. M., Profy, A. T. & Wilson, I. A. (1993) *Structure* **1,** 83–93.
31. Foote, J. & Milstein, C. (1994) *Proc. Natl. Acad. Sci. USA* **91,** 10370–10374.